

Carrier providers or killers: The case of Cu defects in CdTe

Ji-Hui Yang,^{1,a)} Wyatt K. Metzger,¹ and Su-Huai Wei^{2,a)}

¹National Renewable Energy Laboratory, Golden, Colorado 80401, USA

²Beijing Computational Science Research Center, Beijing 100094, China

(Received 1 June 2017; accepted 17 July 2017; published online 26 July 2017)

Defects play important roles in semiconductors for optoelectronic applications. Common intuition is that defects with shallow levels act as carrier providers and defects with deep levels are carrier killers. Here, taking the Cu defects in CdTe as an example, we show that relatively shallow defects can play both roles. Using first-principles calculation methods combined with thermodynamic simulations, we study the dialectic effects of Cu-related defects on hole density and lifetime in bulk CdTe. Because Cu_{Cd} can form a relatively shallow acceptor, we find that increased Cu incorporation into CdTe indeed can help achieve high hole density; however, too much Cu can cause significant non-radiative recombination. We discuss strategies to balance the contradictory effects of Cu defects based on the calculated impact of Cd chemical potential, copper defect concentrations, and annealing temperature on lifetime and hole density. These findings advance the understanding of the potential complex defect behaviors of relatively shallow defect states in semiconductors.

Published by AIP Publishing. [<http://dx.doi.org/10.1063/1.4986077>]

Defects play important roles in the electro-optical properties of semiconductors, which are critical for applications such as detectors and photovoltaics (PV).^{1,2} Generally speaking, there are two important kinds of defects. On the one hand, defects with shallow defect transition energy levels can provide free carriers by ionization, which contribute to solar cell open-circuit voltage (V_{oc}) and fill factor.^{3,4} On the other hand, defects, especially those with deep transition energy levels, can cause non-radiative Shockley-Read-Hall (SRH) recombination of photo-generated electrons and holes, thereby decreasing photo-current, fill factor, and V_{oc} .⁵ In general, these two kinds of defects are different and a common approach to improve solar cell performance is to increase the carrier providers and decrease the lifetime killers.

However, as the concentration of any defect increases, it will contribute more to recombination based on the relation $\tau = (B_D N_D)^{-1}$, where τ is the carrier lifetime, B_D is the defect carrier capture rate, and N_D is the defect density. In this case, a contradiction arises where an increased shallow defect density can increase the carrier concentration but also increase non-radiative recombination. This contradictory behavior can be more prominent in II-VI materials because the acceptors often have defect transition energy levels >0.1 eV above the valence band maximum (VBM) and carrier compensation is common. When there is strong compensation between donor and acceptor defects, more defects have to be created to achieve a certain carrier concentration. In some cases, the defect concentration can be several orders of magnitude greater than the carrier concentration. When this happens, the non-radiative recombination induced by defects even with relatively shallow defect levels can be significant and limit device performance. Consequently, optimization must balance the advantageous and deleterious impacts of these defects. Here, we show that Cu doping in CdTe is such a situation.

CdTe is one of the leading thin-film solar cell materials; recently, First Solar achieved a world-record cell efficiency of 22.1%.⁶ Experimentally, Cu is crucial to attain a relatively high hole density and thus efficiency. However, the exact roles of Cu in enhancing and even limiting CdTe solar cell efficiency are not yet well understood. It has been reported that Cu can reduce the back contact barrier,^{7,8} enhance CdTe p -type doping, and modify carrier lifetime.^{9–11} Recent experiments also show that Cu-related defects can cause non-radiative recombination of photo-generated carriers.^{12,13} In addition, because Cu is a mobile species, its concentration and defect nature can change during operation, creating metastability and degradation effects.^{14,15} Due to its important roles, it is of great interest to clarify whether and how Cu-related defects can act as both carrier providers and carrier killers. This can also provide insight into the dialectic roles of somewhat shallow semiconductor defects.

Here, we use first-principles calculations and thermodynamic simulations to examine the impact of Cu-related defects in bulk CdTe. The calculations are performed using the density-functional theory (DFT) as implemented in the VASP code,^{16,17} with the detailed methodology described in Ref. 20. The calculated chemical potential conditions are $\mu_{Cd} + \mu_{Te} = \Delta H_f(CdTe) = -1.17$ eV and $\mu_{Cu} + \mu_{Te} \leq \Delta H_f(CuTe) = -0.25$ eV, where $\Delta H_f(CdTe)$ and $\Delta H_f(CuTe)$ are the formation enthalpies of perfect CdTe and CuTe bulks, respectively. For simplicity and practical reasons, here we focus on Cu on Cd sites and Cu interstitials because other Cu-related defects and intrinsic CdTe defects are less dominant.¹⁸

The calculated defect formation energies of Cu_{Cd} and Cu_i as functions of Fermi levels are shown in Fig. 1, where two chemical potential conditions are considered. In Fig. 1(a), for an extremely Cd-poor condition ($\mu_{Cd} = -1.17$), Cu_{Cd} always has smaller formation energy than Cu_i, so their compensation is very weak. Figure 1(b) indicates that in a slightly Cd-rich condition ($\mu_{Cd} = -0.57$), Cu_{Cd} can be strongly compensated by Cu_i when the Fermi level is close to the crossing point of their formation energy lines. The (0/−)

^{a)}Electronic addresses: jihuiyang2016@gmail.com and suhuaiwei@csr.ac.cn

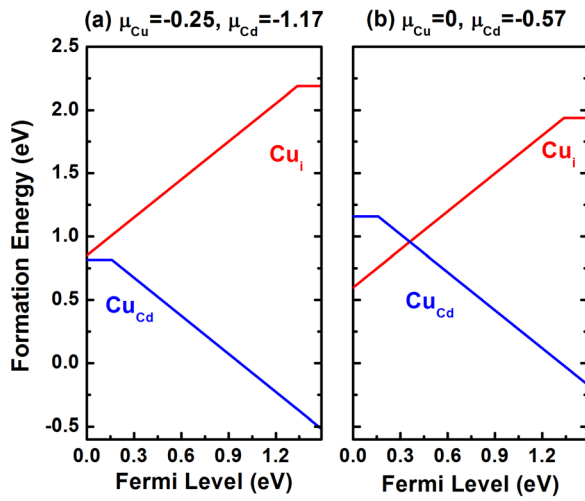


FIG. 1. HSE06 calculated formation energies of Cu_{Cd} and Cu_i as functions of Fermi levels (referenced to the VBM) under (a) extremely Cd-poor and (b) slightly Cd-rich conditions.

transition energy level of Cu_{Cd} is calculated to be 0.16 eV above the VBM of CdTe using Heyd-Scuseria-Ernzerhof (HSE06) hybrid functionals,¹⁹ in good agreement with experimental measurements.¹³ The (0/+) transition energy level of Cu_i is 0.15 eV below the CdTe conduction band minimum (CBM).

Although these defect levels are close to the band edges, their in-gap positions indicate that they can still be involved in non-radiative recombination. Here, we have quantitatively calculated the non-radiative recombination rates of these two defects using the recently developed method that takes into account multiphonon emissions under static approximations.^{20,21} This method has shown very consistent results with experiments on II-VI and III-V semiconductors.^{21,22} We calculate both the electron and hole transition rates for Cu_{Cd} and Cu_i . For the electron capture rate, our calculated results at $T = 300$ K are $2.55 \times 10^{-10} \text{ cm}^3 \text{ s}^{-1}$ and $9.96 \times 10^{-9} \text{ cm}^3 \text{ s}^{-1}$ for Cu_{Cd} and Cu_i , respectively. For the hole capture rate, the results are $2.84 \times 10^{-8} \text{ cm}^3 \text{ s}^{-1}$ and $6.82 \times 10^{-10} \text{ cm}^3 \text{ s}^{-1}$ for Cu_{Cd} and Cu_i , respectively.

One might expect more difference for the large energy transitions, such as the 0.16 eV Cu_{Cd} acceptor capturing an electron from the conduction band. However, because Cu_{Cd} mainly has Cu d and Te p orbital character, it can strongly couple with the CBM, which mainly has s orbital character, leading to the significant electron trapping. Similarly, Cu_i mainly has s orbital character and can strongly couple with the VBM, which has p and d orbital characters, leading to significant hole trapping.

The recombination process is generally limited by the slow step. Considering the electron and hole densities at the carrier injection level caused by sunlight in CdTe solar cells,²² the recombination rate due to Cu_{Cd} is largely determined by the electron trapping process and the rate due to Cu_i is determined largely by the hole trapping process. Compared to the trapping rate of the dominant intrinsic recombination center $\text{Te}_{\text{Cd}}^{2+}$,²² the electron trapping rate of Cu_{Cd} and the hole trapping rate of Cu_i are two or three orders of magnitude smaller, i.e., $10^{-7} \text{ cm}^3 \text{ s}^{-1}$ for $\text{Te}_{\text{Cd}}^{2+}$ versus $10^{-10} \text{ cm}^3 \text{ s}^{-1}$ for these Cu defects. The small trapping rates

of Cu defects are expected from their relatively shallow defect levels compared to the bandgap of CdTe but are still significant in light of significant Cu incorporation in practice.

Once the trapping rates are known, the cross-section can be obtained by $\sigma = B/v$, where σ is the cross section, B is the trapping rate, and v is the carrier velocity. If we assume that v is 10^7 cm/s , the Cu_{Cd} electron and hole capture cross sections are estimated to be $2.55 \times 10^{-17} \text{ cm}^2$ and $9.96 \times 10^{-16} \text{ cm}^2$, respectively, and the electron and Cu_i hole capture cross sections are estimated to be $2.84 \times 10^{-15} \text{ cm}^2$ and $6.82 \times 10^{-17} \text{ cm}^2$, respectively. The calculated results are in good agreement with recent experimental work, which is estimated on the order of 10^{-16} cm^2 .¹³

The Cu_{Cd} and Cu_i SRH lifetimes are given as $\tau_{\text{Cu}_{\text{Cd}}} = (B_n N_{\text{Cu}_{\text{Cd}}})^{-1}$ and $\tau_{\text{Cu}_i} = (B_p N_{\text{Cu}_i})^{-1}$, with B_n and B_p being the electron and hole trapping rates, respectively. Despite the small trapping rates, Cu defects can still cause significant recombination if the Cu concentration is high. For example, if the total concentration of Cu defects is larger than 10^{17} cm^{-3} , the SRH carrier lifetime τ will be smaller than tens of nanoseconds determined from $\frac{1}{\tau} = \frac{1}{\tau_{\text{Cu}_{\text{Cd}}}} + \frac{1}{\tau_{\text{Cu}_i}}$ and further decrease to several nanoseconds if the Cu concentration exceeds 10^{18} cm^{-3} .

Consequently, a contradictory consideration of hole density and carrier lifetime arises: from the perspective of obtaining a high hole density (i.e., $\geq 10^{16} \text{ cm}^{-3}$), a large Cu incorporation is preferred; from the perspective of obtaining a high carrier lifetime, less Cu incorporation is preferred. In practice, Cu amounts can be controlled by the incorporation method, annealing temperatures, Cd chemical potentials, and other factors such as diffusion times. To get a high hole density, the extremely Cd-poor condition and a high annealing temperature are beneficial because more Cu_{Cd} defects can be created. To get a high carrier lifetime and avoid excessive Cu levels, the not-so-poor Cd condition and a low annealing temperature are helpful.

Due to the complex roles of the annealing temperature and the Cd chemical potential in determining the optimal Cu conditions, we perform thermodynamic simulations. First, we consider the case when Cu is under thermodynamic equilibrium. Under this condition and within the dilute limit, the density of a defect α with charge state q is assumed to reach equilibrium at the incorporation temperature and can be determined from

$$n(\alpha, q) = N_{\text{site}} g_q e^{-\frac{\Delta H_f(\alpha, q)}{k_B T}}, \quad (1)$$

where N_{site} is the number of possible sites per volume for defect α , g_q is the degeneracy factor,^{23,24} and $\Delta H_f(\alpha, q)$ is the defect formation energy²⁵ defined as

$$\Delta H_f(\alpha, q) = E(\alpha, q) - E(\text{host}) + \sum_i n_i (E_i + \mu_i) + q [E_{\text{VBM}}(\text{host}) + E_F], \quad (2)$$

which is a function of chemical potentials μ_i of involved elements and E_F . At a given temperature, the thermally excited electron density n_0 and hole density p_0 are also functions of the Fermi level, which are given as

$$n_0 = N_c e^{-\frac{E_c - E_F}{k_B T}}, \quad N_c = 2 \frac{(2\pi m_n^* k_B T)^{3/2}}{h^3},$$

$$p_0 = N_v e^{-\frac{E_F - E_v}{k_B T}}, \quad N_v = 2 \frac{(2\pi m_p^* k_B T)^{3/2}}{h^3}. \quad (3)$$

Here, N_c is the temperature-dependent effective density of states (DOS) of the conduction band and N_v is the effective DOS of the valence band. m_n^* (0.095 m_0 for CdTe) and m_p^* (0.84 m_0 for CdTe) are effective masses of electrons and holes.²⁶ The charge neutralization condition for Cu-doped CdTe requires

$$p_0 + n(\text{Cu}_i^+) = n_0 + n(\text{Cu}_{\text{Cd}}^-). \quad (4)$$

By solving Eqs. (1)–(4) self-consistently, we can obtain the Cu defect densities in CdTe at given chemical potentials, as well as carrier densities and Fermi levels assuming that everything reaches equilibrium at a given temperature. Figure 2 shows our simulation results for extremely Cd-poor and slightly Cd-rich conditions at $T = 300$ K, which clearly indicates that Cu_i and Cu_{Cd} sites may fully compensate one another for slightly Cd-rich conditions, so that increasing the Cu amount does not significantly increase hole density but does decrease the lifetime. On the other hand, very Cd-poor conditions indicate increasing hole density with the Cu concentration as Cu preferentially fills Cd rather than interstitial sites.

In reality, the Cu annealing temperature is often well above room temperature and then the system is cooled down to 300 K. During the annealing process, it is reasonable to assume that if the cooling rate is high, the amount of Cu at substitutional sites and the amount of Cu interstitials are similar to those of the high annealing temperature,²⁷ although their charge states might be redistributed following the Boltzmann distributions. For example, the Cu_{Cd} defect can be redistributed between its neutral and -1 states by

$$n(\text{Cu}_{\text{Cd}}^0) = N_{\text{Cu}_{\text{Cd}}} \times \frac{g_0 e^{-\Delta H_f(\text{Cu}_{\text{Cd}}^0)/k_B T}}{g_0 e^{-\Delta H_f(\text{Cu}_{\text{Cd}}^0)/k_B T} + g_{-1} e^{-\Delta H_f(\text{Cu}_{\text{Cd}}^-)/k_B T}};$$

$$n(\text{Cu}_{\text{Cd}}^-) = N_{\text{Cu}_{\text{Cd}}} \times \frac{g_{-1} e^{-\Delta H_f(\text{Cu}_{\text{Cd}}^-)/k_B T}}{g_0 e^{-\Delta H_f(\text{Cu}_{\text{Cd}}^0)/k_B T} + g_{-1} e^{-\Delta H_f(\text{Cu}_{\text{Cd}}^-)/k_B T}}, \quad (5)$$

where $N_{\text{Cu}_{\text{Cd}}}$ is the total density of Cu at Cd substitutional sites in CdTe calculated at the high incorporation temperature; g_0 and g_{-1} are the degeneracy factors, which are 4 and 1 for Cu_{Cd}^0 and Cu_{Cd}^- , respectively; and $\Delta H_f(\text{Cu}_{\text{Cd}}^0)$ and $\Delta H_f(\text{Cu}_{\text{Cd}}^-)$ are the defect formation energies. By solving Eqs. (2)–(5) at room temperature using the defect information at the high annealing temperature, we can estimate the room-temperature Cu defect densities in CdTe as well as carrier densities and Fermi levels at given chemical potentials.

We perform simulations over a wide range of annealing temperatures. The obtained hole density, Fermi level, defect density, and carrier lifetime after annealing samples at elevated temperatures and quickly cooling to room temperature are shown in Fig. 3. At given Cd and Cu chemical potential conditions, the Cu concentration monotonically increases with temperature [Figs. 3(b) and 3(e)] because more defects can be created at a higher temperature. At the same time, the hole density monotonically increases and the Fermi level monotonically decreases at extremely Cd-poor conditions when the annealing temperature increases [Fig. 3(a)]. This trend occurs because the band-edge thermal excitation at finite temperatures always tends to drag the Fermi level to the middle of the bandgap, where Cu_{Cd} always has lower formation energy than Cu_i . As a result, more Cu_{Cd} will be created than Cu_i with increased annealing temperature. After annealing, although some Cu_{Cd} defects will convert from negatively charged states to neutral states, the net density difference between Cu_{Cd}^- and Cu_i^+ still increases with increased annealing temperature, resulting in increased hole density and decreased Fermi level. The results at slightly

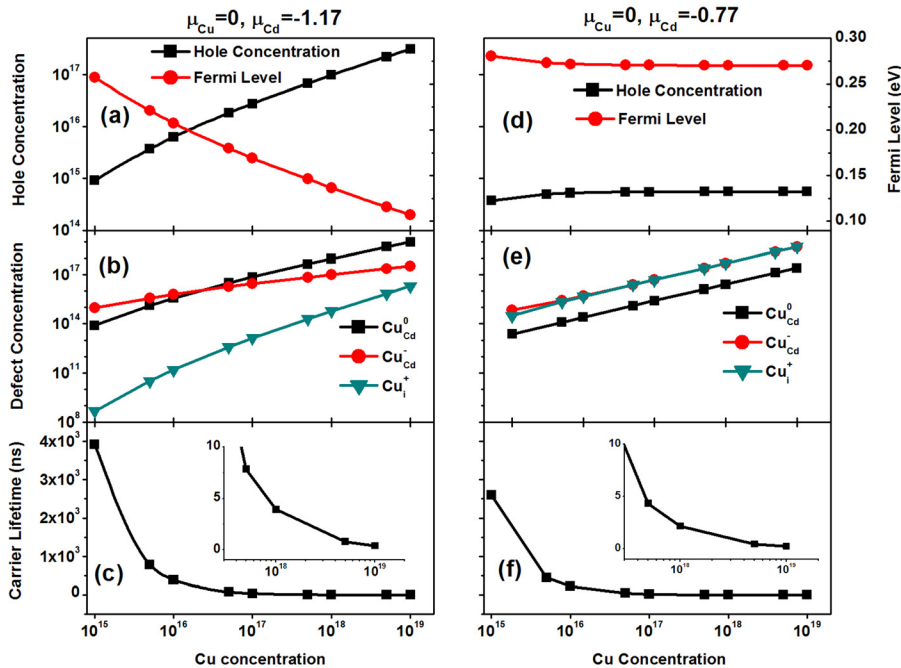


FIG. 2. (a) and (d) Fermi level and hole density, (b) and (e) Cu defect densities, and (c) and (f) SRH carrier lifetime in Cu doped CdTe as a function of incorporated Cu concentration under the thermodynamic equilibrium condition at $T = 300$ K for the extremely Cd-poor case (left panel) and slightly Cd-poor case (right panel).

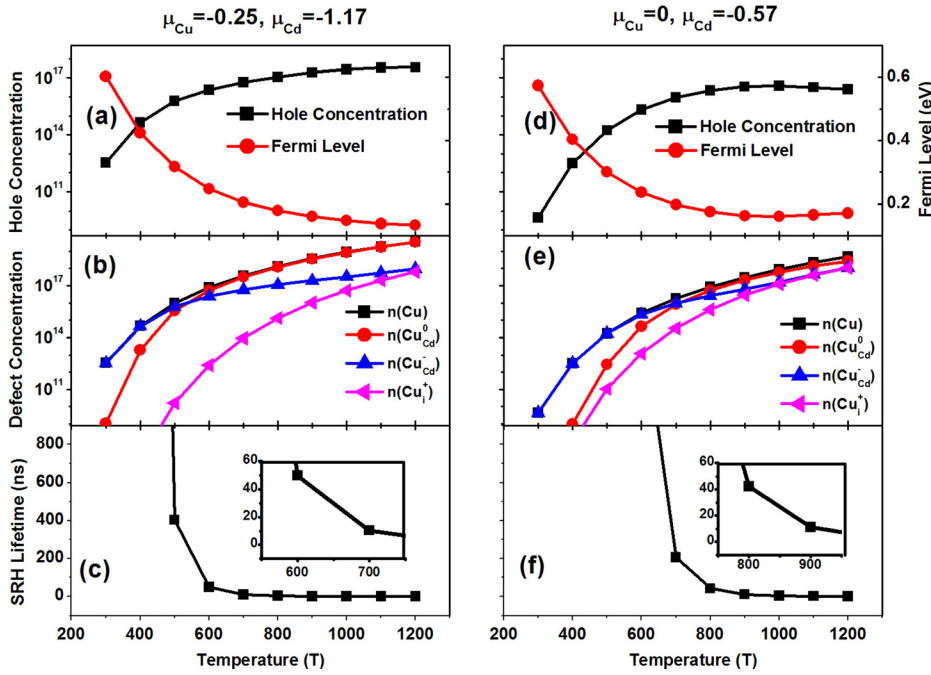


FIG. 3. (a) and (d) Fermi level and hole density, (b) and (e) Cu defect densities, and (c) and (f) SRH carrier lifetime (due to Cu only) after annealing Cu doped CdTe at different temperatures under the thermodynamic equilibrium condition to $T = 300$ K for the extremely Cd-poor case (left panel) and slightly Cd-rich case (right panel).

Cd-rich conditions are a little different. In this case, the formation energy difference between Cu_{Cd} and Cu_i is smaller. Although more Cu_{Cd} will be created than Cu_i at the higher annealing temperature, their density difference decreases. After annealing, partial conversion of Cu_{Cd}^- defects into its neutral states further reduces the net density difference between Cu_{Cd}^- and Cu_i^+ . The consequence is that the hole density and Fermi level begin to decrease if the annealing temperature exceeds about 900–1000 K in Fig. 3(d). At a given annealing temperature, the Cu concentration and the resulting hole density decrease when Cd chemical potential increases from the extremely Cd-poor condition to the slightly Cd-rich condition. This is because the formation energy of Cu_{Cd} increases, and thus, less Cu_{Cd} can be created to contribute to the hole density when the Cd chemical potential increases. Similarly, the Fermi level increases with the increase in Cd chemical potential.

Our simulations confirm that the higher annealing temperature and the extremely Cd-poor condition are indeed helpful to get higher hole density. However, the incorporated Cu concentration can be too excessive and cause significant non-radiative recombination. For example, with the incorporation temperature $T = 800$ K under extremely Cd-poor conditions, $\sim 10^{18} \text{ cm}^{-3}$ Cu can be incorporated into CdTe and the hole density can reach $\sim 10^{17} \text{ cm}^{-3}$. However, the carrier lifetime meanwhile is limited to several nanoseconds. Experiments examining Cu hole density and lifetime after annealing Cu-diffused CdTe at high temperatures in Te overpressures have achieved hole density greater than 10^{16} cm^{-3} but exhibited a sharp decrease in lifetime.²⁸ Therefore, in practice, one needs to balance the hole density and the carrier lifetime by optimally matching the incorporation temperature and the Cd chemical potential. Experimentally, it is known that a high hole density above 10^{16} cm^{-3} with a carrier lifetime of tens of nanoseconds is sufficient to approach V_{oc} of 1 V.²⁹

Contrary to intuition, a higher annealing temperature and extremely Cd-poor condition are actually not necessary to realize the optimal Cu defect chemistry. Using the

thermodynamic simulation methods, we try different combinations of the annealing temperatures and Cd chemical potentials. Those combinations that can enable both a high hole density above 10^{16} cm^{-3} and a carrier lifetime of tens of nanoseconds are shown in Fig. 4. During our simulations, we allow the hole density and the carrier lifetime to vary by one order of magnitude, which gives the variation of Cd chemical potentials within about 0.1 eV, as indicated by the error bars in Fig. 4. Generally speaking, a lower incorporation temperature is needed with more Cd-poor stoichiometry. Our simulations thus offer a theoretical guide on how to optimally choose the annealing temperatures and the Cd chemical potentials under thermodynamic equilibrium conditions.

In practice, a critical component of controlling the Cu balance in CdTe is to control the total amount of Cu concentration, i.e., by controlling the amount of Cu diffusion sources and the diffusion times. The Cu will be distributed into

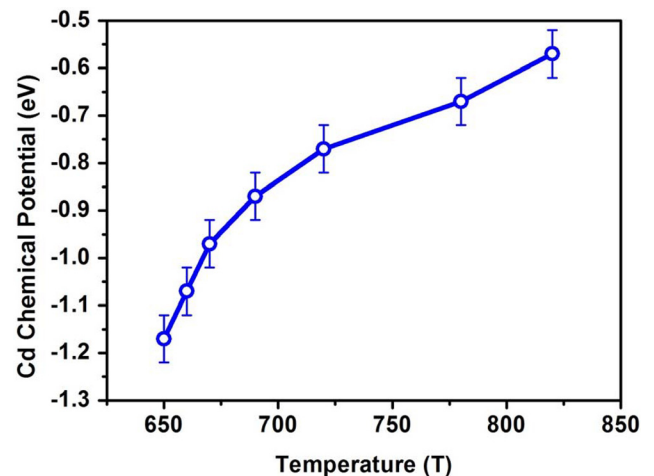


FIG. 4. The estimated optimal match between the Cu annealing temperature and the Cd chemical potential to achieve both a high hole density of above 10^{16} cm^{-3} and a carrier lifetime that can exceed 10 ns. The error bars indicate our estimation.

different Cu defects following the Boltzmann distributions similar to Eq. (5) except that now the total Cu density N_{Cu} is distributed into Cu_{Cd}^0 , Cu_{Cd}^- , Cu_i^0 , and Cu_i^+ according to their weights determined from their defect formation energies. Our above simulations indicate that a reasonable Cu concentration in CdTe for PV applications is about 10^{17} cm^{-3} , which is sufficient to provide a hole density above 10^{16} cm^{-3} and retain the carrier lifetimes of ten of nanoseconds (assuming other recombination mechanisms do not limit lifetime). More Cu incorporation will reduce the carrier lifetime and less Cu incorporation cannot achieve a high hole density.

While this strategy is not necessarily restricted to equilibrium growth conditions, the final hole density and carrier lifetime are still determined by the incorporation temperature and Cd chemical potential. To examine this, we perform thermodynamic simulations over a wide range of incorporation temperatures and Cd chemical potentials with the total amount of Cu now fixed at 10^{17} cm^{-3} . Figure 5 indicates that the carrier lifetimes are always larger than 20 ns due to the limited Cu incorporation. In addition, to achieve a high hole density at the extremely Cd-poor condition, a low temperature of 300–400 K is sufficient [Fig. 5(b)]. However, with increased Cd chemical potential, a higher annealing temperature is necessary. For example, under the slightly Cd-rich condition in the case of Fig. 1(b), an annealing temperature of about 800 K is required to get a hole density above 10^{16} cm^{-3} . In fact, for a wide range of Cd chemical potentials, we can often get hole density $\geq 10^{16} \text{ cm}^{-3}$ and a carrier lifetime of nearly 40 ns [Fig. 5(c)] as long as the total Cu concentration is limited to $\sim 10^{17} \text{ cm}^{-3}$. Again, our simulations show that a higher incorporation temperature and extremely Cd-poor chemical potential are not necessary to realize the optimal Cu defect chemistry. Instead, the total Cu concentration in CdTe and a good match between the anneal temperature and the Cd chemical potentials are important. In practice, it should be noted that during cooling, storage, and device operation, the equilibrium may vary due to experimental issues and because the barrier for Cu transitioning from a Cd site to an interstitial site is small.¹⁸ Consequently, the hole density and lifetime may adjust leading to stability issues.

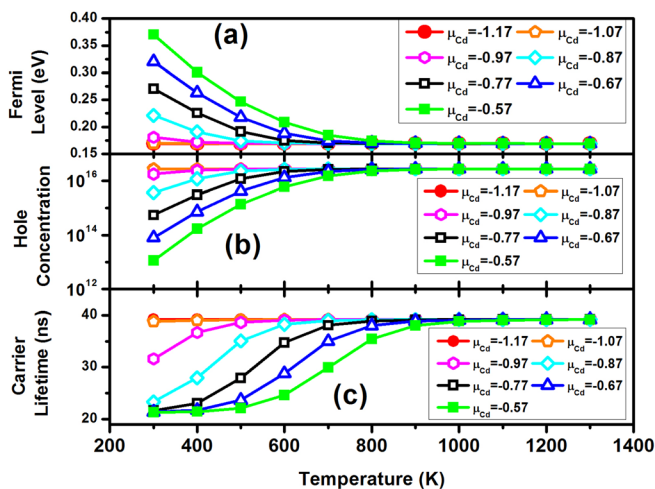


FIG. 5. (a) Fermi level, (b) hole density, and (c) SRH carrier lifetime (Cu only) in annealed CdTe samples after annealing CdTe samples from different Cu annealing temperatures to $T = 300 \text{ K}$ for different Cd chemical potentials. The total amount of Cu is fixed as 10^{17} cm^{-3} .

In conclusion, we have studied the roles of Cu-related defects in bulk CdTe. In general, opposing trends exist between lifetime and hole density with Cu incorporation. To optimize the Cu doping and lifetime in CdTe, the total amount of Cu incorporated, the annealing temperature, and the Cd chemical potential are critical. The findings provide insight into the dialectic roles of Cu defects for CdTe solar technology and more generally the potential dialectic behaviors for somewhat shallow defects in semiconductors for optoelectronic applications.

This work was funded by the U.S. Department of Energy, EERE/SunShot program, under Contract Nos. DE-AC36-08GO28308 and DE-EE0006344. Work at Beijing CSRC was supported by Science Challenge Project, No. TZ20160003, and NSAF joint program under Grant No. U1530401. The calculations are done on NREL's Peregrine supercomputer and NERSC's supercomputer.

- ¹W.-J. Yin, T. Shi, and Y. Yan, *Appl. Phys. Lett.* **104**, 063903 (2014).
- ²S. Chen, X. G. Gong, A. Walsh, and S.-H. Wei, *Appl. Phys. Lett.* **96**, 021902 (2010).
- ³J. Sites and J. Pan, *Thin Solid Films* **515**, 6099 (2007).
- ⁴A. Kanevce and T. A. Gessert, *IEEE J. Photovoltaics* **1**, 99 (2011).
- ⁵P. Würfel, *Physics of Solar Cells: From Principles to New Concepts* (Wiley-VCH Verlag, Weinheim, 2005), p. 71.
- ⁶See http://www.nrel.gov/ncpv/images/efficiency_chart.jpg for Best Research-Cell Efficiencies.
- ⁷D. H. Rose, F. S. Hasoon, R. G. Dhere, D. S. Albin, R. M. Ribelin, X. S. Li, Y. Mahathongdy, T. A. Gessert, and P. Sheldon, *Prog. Photovoltaics: Res. Appl.* **7**, 331 (1999).
- ⁸E. I. Adirovich, Yu. M. Yuabov, and G. R. Yagudaev, *Sov. Phys. Semicond.* **3**, 61 (1969).
- ⁹L. Kranz, C. Gretener, J. Perrenoud, R. Schmitt, F. Pianezzi, F. L. Mattina, P. Blösch, E. Cheah, A. Chirilă, C. M. Fella, H. Hagendorfer, T. Jäger, S. Nishiwaki, A. R. Uhl, S. Buecheler, and A. N. Tiwari, *Nat. Commun.* **4**, 2306 (2013).
- ¹⁰J. Perrenoud, L. Kranz, C. Gretener, F. Pianezzi, S. Nishiwaki, S. Buecheler, and A. N. Tiwari, *J. Appl. Phys.* **114**, 174505 (2013).
- ¹¹T. A. Gessert, W. K. Metzger, P. Dippo, S. E. Asher, R. G. Dhere, and M. R. Young, *Thin Solid Films* **517**, 2370 (2009).
- ¹²S. H. Demtsu, D. S. Albin, J. R. Sites, W. K. Metzger, and A. Duda, *Thin Solid Films* **516**, 2251 (2007).
- ¹³D. Kuciauskas, P. Dippo, A. Kanevce, Z. Zhao, L. Cheng, A. Los, M. Gloeckler, and W. K. Metzger, *Appl. Phys. Lett.* **107**, 243906 (2015).
- ¹⁴C. R. Corwine, A. O. Pudov, M. Gloeckler, S. H. Demtsu, and J. R. Sites, *Sol. Energy Mater. Sol. Cells* **82**, 481 (2004).
- ¹⁵D. S. Albin, "Accelerated stress testing and diagnostic analysis of degradation in CdTe solar cells," *Proc. SPIE* **7048**, 70480N (2008).
- ¹⁶G. Kresse and J. Furthmüller, *Phys. Rev. B* **54**, 11169 (1996).
- ¹⁷G. Kresse and J. Furthmüller, *Comput. Mater. Sci.* **6**, 15 (1996).
- ¹⁸J.-H. Yang, W.-J. Yin, J.-S. Park, J. Ma, and S.-H. Wei, *Semicond. Sci. Technol.* **31**, 083002 (2016).
- ¹⁹J. Heyd, G. E. Scuseria, and M. Ernzerhof, *J. Chem. Phys.* **118**, 8207 (2003).
- ²⁰L. Shi and L.-W. Wang, *Phys. Rev. Lett.* **109**, 245501 (2012).
- ²¹L. Shi, K. Xu, and L.-W. Wang, *Phys. Rev. B* **91**, 205315 (2015).
- ²²J.-H. Yang, L. Shi, L.-W. Wang, and S.-H. Wei, *Sci. Rep.* **6**, 21712 (2016).
- ²³S. Sze, *Physics of Semiconductor Devices*, 2nd ed. (Wiley, New York, 1981).
- ²⁴J. Ma, S.-H. Wei, T. A. Gessert, and K. K. Chin, *Phys. Rev. B* **83**, 245207 (2011).
- ²⁵S.-H. Wei, *Comput. Mater. Sci.* **30**, 337 (2004).
- ²⁶R. Romestain and C. Weisbuch, *Phys. Rev. Lett.* **45**, 2067 (1980).
- ²⁷J.-H. Yang, J.-S. Park, J. Kang, W. Metzger, T. Barnes, and S.-H. Wei, *Phys. Rev. B* **90**, 245202 (2014).
- ²⁸J. M. Burst, S. B. Farrell, D. S. Albin, E. Colegrove, M. O. Reese, J. N. Duenow, D. Kuciauskas, and W. K. Metzger, *APL Mater.* **4**, 116102 (2016).
- ²⁹J. M. Burst, J. N. Duenow, D. S. Albin, E. Colegrove, M. O. Reese, J. A. Aguiar, C.-S. Jiang, M. K. Patel, M. M. Al-Jassim, D. Kuciauskas, S. Swain, T. Ablekim, K. G. Lynn, and W. K. Metzger, *Nat. Energy* **1**, 16015 (2016).